Universal Decoherence under Gravity: A Perspective through the Equivalence Principle

Belinda H. Pang, Yanbei Chen, and Farid Ya. Khalili

Phys. Rev. Lett. **117**, 090401 — Published 24 August 2016

DOI: 10.1103/PhysRevLett.117.090401

On universal decoherence under gravity: a perspective through the Equivalence Principle

Belinda Pang and Yanbei Chen
Burke Institute for Theoretical Physics and the Institute for Quantum Information and Matter, M/C 350-17, California Institute of Technology, Pasadena, California 91125

Farid Ya. Khalili
Moscow State University, Faculty of Physics, Moscow 119991, Russia

In Nature Phys. 11, 668 (2015) (Ref. [1]), a composite particle prepared in a pure initial quantum state and propagated in a uniform gravitational field is shown to undergo a decoherence process at a rate determined by the gravitational acceleration. By assuming Einstein's Equivalence Principle to be valid, we analyze a physical realization of the (1+1)d thought experiment of Ref. [1] to demonstrate that the dephasing between the different internal states arise not from gravity but rather from differences in their rest mass, and the mass dependence of the de Broglie wave's dispersion relation. We provide an alternative view to the situation considered by Ref. [1], where we propose that gravity plays a kinematic role by providing a relative velocity to the detector frame with respect to the particle; visibility can be easily recovered by giving the screen an appropriate uniform velocity. We then apply this insight to their thought experiment in (1+1)d to draw a direct correspondance, and obtain the same mathematical result for dephasing. We finally propose that dephasing due to gravity may in fact take place for certain modifications to the gravitational potential where the Equivalence Principle is violated.

Introduction.– Exciting ideas have recently been proposed to explore the interplay between quantum mechanics and gravity using precision measurement experiments, for example testing the quantum evolution of self-gravitating objects [2], searching for modifications to the canonical commutation relation [3], and studying the propagation of quantum wavefunctions in an external gravitational field [4, 5]. There have also been proposals for the emergence of classicality through gravitationally induced decoherence, such as from an effective field theory approach [6], [7] or the Diósi-Penrose model [8], [9]. Pikovski et al. recently pointed out that a composite quantum particle, prepared in an initial product state between its "center of mass" and its internal state, will undergo a decoherence process with respect to its spatial degrees of freedom in a uniform gravitational field — as exhibited by a loss of contrast in matter-wave interferometry experiments, whose loss depends on the gravitational acceleration g [1]. They attributed this effect to gravitational time dilation, and proposed this as a universal decoherence mechanism for composite particles. This interpretation has significant implications and has been the subject of lively debate [10–13].

According to Einstein's Equivalence Principle (EEP), freely falling experiments cannot detect the magnitude of gravitational acceleration [14]. Of course, the thought experiment in Ref. [1] is not in free fall: although there is no physical detector in their setup, implicitly their detection process occurs in an accelerating lab. This means their result is not necessarily in contradiction with the EEP. Nevertheless, it is still interesting to explain why the dephasing, which takes place during the particle's *free propagation*, has a rate determined by gravity. Furthermore, since EEP implies that gravity is equivalent to acceleration, the idea of decoherence induced by uniform gravity suggests that the motion of an accelerated observer affects the evolution of a quantum system in such a way that causes decoherence, which is an idea that begs clarification.

At this point, we note that calculating the dephasing of wavefunctions in the Lab frame as in Ref. [1] mixes the observed effects due to propagation and those due to acceleration of the detection frame. In this paper, we will separate these two processes by providing a description of both the system and measurement process in free falling Lorentz frames which can be extended globally to Minkowski coordinates. In a Lorentz frame, the internal states of the composite particle do not interact with external potentials or each other, and are distinguished only by their rest mass m. Therefore we can treat each internal state as an independent, freely propagating particle species labeled by m. The particles are measured in a detector frame with relative motion, where specializing to a uniformly accelerating detector frame recovers the case of gravity. The overall measurement outcome is the trace over all species. Using this framework, we model a physical realization of the (1+1)d thought experiment of Ref. [1]. In (3+1)d, we consider a particle beam propagating along one direction, being measured by a screen travelling along an arbitrary trajectory in a transverse direction [Fig. 1]. Due to the mass dependence of de Broglie wave dispersion, where $\omega_k \approx k^2/2m$, the packets have different propagation velocities and will arrive at the detector at different times. This means that the pattern registered by the *moving* detector for each species will be spatially shifted along the direction of detector motion [Fig. 2]. This is equivalent to a mass dependent phase shift that will result in the blurring of interference fringes when all patterns are summed. Here, the motion of the detector will determine the size of spatial the shifts, and therefore determines how much blurring occurs. This explains the appearance of g in the dephasing rate of Ref. [1], since it controls the motion of the screen for the case of uniform gravity.

In this view, the source of dephasing is mass dependent dispersion, which appears as a loss of quantum coherence due to a *kinematic* effect of detector motion. To emphasize that it is not gravitational, we predict dephasing even in the absence of gravity for a detector with uniform velocity. This insight allows us to understand the thought experiment of Ref. [1] without referring to time dilation: there, the interference pattern generated by each species has a mass dependent spatial wavevector, again due to dispersion. The dephasing is larger as one moves farther away from the center of the superposition. If we observe the state at a constant coordinate position in the Lab frame, then the effect of a moving Lab move farther away from its center. Mathematically, this corresponds to Ref. [1]'s calculation of the correlations between constant coordinate values z_1 and z_2, initially near the center, at some later time in the Lab frame. Therefore g again appears in the dephasing rate via the Lab frame's motion.

The Lorentz frame approach provides a simple way to understand the dephasing. However, a rigorous calculation requires a description of the system and measurement as Lorentz covariants, since Lorentz symmetry is a property required in our discussion of frame independent physics viewed by arbitrary observers. We develop our formalism in this fully relativistic way, although we find that relativistic effects are ignorable, and the non-relativistic limit completely reconstructs the effect found in Ref. [1]. In this analysis we have assumed EEP to hold. We point out comparison of this approach with an explicit treatment of gravity as an modified external force field offers possibilities to test for EEP violations in the quantum regime. For our calculations and results we have set $\hbar = c = 1$.

Evolution of a Composite Particle in the Lorentz Frame.– Here, we give a Lorentz covariant description of the composite particle, then examine its evolution in a Lorentz frame with Cartesian coordinates $x^\mu = (t, x, y, z) = (t, \mathbf{x})$. We model each species as an independent Klein Gordon field, with its field operator $\hat{\phi}_m(x^\mu)$ satisfying $(\Box + m^2)\hat{\phi}_m = 0$, and with the relativistic dispersion relation $\omega_m(\mathbf{k}) = \sqrt{m^2 + \mathbf{k}^2}$, which we emphasize is mass dependent. Without loss of generality, a single particle state for species m is given by

$$|\Psi_m\rangle = \int \frac{d^3\mathbf{k}}{(2\pi)^3}\, g_m(\mathbf{k})\hat{a}^\dagger_m(\mathbf{k})|0\rangle \qquad (1)$$

where $\hat{a}^\dagger_m(\mathbf{k})$ is the creation operator associated with $\hat{\phi}_m$, and creates a momentum eigenstate in the quantization frame with eigenvalue $\mathbf{k}$. When g_m is limited to values of $|\mathbf{k}| \ll m$, the quantum state is non-relativistic. The Lorentz covariant state vector can then be mapped to the time dependent quantum mechanical wavefunction $\psi_m(t, \mathbf{x})$ for a chosen frame by constructing the non-relativistic field operator $\hat{\Phi}(t, \mathbf{x}) = e^{imt}\hat{\phi}(t, \mathbf{x})$ and noting that $\psi_m(t, \mathbf{x}) = \langle 0|\hat{\Phi}(t, \mathbf{x})|\Psi_m\rangle$. Conversely, given the form of the initial wavefunction $\psi_m(0, \mathbf{x})$ in the particle emitter frame, we can identify the state vector $|\Psi_m\rangle$. Suppose then that the initial state of composite particle is a *direct-product* state between the internal and translational modes of the composite particle. The translational mode corresponds to the "center of mass" degree of freedom of Ref. [1], and contains all the information about the particle's location. Therefore, all species share the same initial wavefunction, or $\psi_m(0, \mathbf{x}) = \psi_{\rm ini}(\mathbf{x})$ (Fig. 1). This implies that they also share the same momentum space distribution, which we denote by $f_m(\mathbf{k})$. We note that $f_m(\mathbf{k}) = g_m(\mathbf{k})/\sqrt{2\omega_m(\mathbf{k})}$.

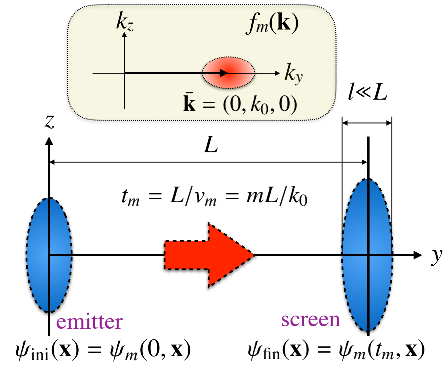

FIG. 1: Propagation of a wavepacket for species m from the emitter to the screen in the Lorentz frame. For each m, the same initial wavefunction leads to the same measured wavefunction on the $y = L$ plane (where the screen is located), but the arrival time of the packets depend on m. Here the screen is moving along z. The inset illustrates that $f_m(\mathbf{k})$ is localized around $\bar{\mathbf{k}}$. For snapshots in time, see left panels of Fig. 2.

We consider the case where $\psi_{\rm ini}(\mathbf{x})$ is spatially localized around the origin and $f_m(\mathbf{k})$ is localized near $\bar{\mathbf{k}} = (0, k_0, 0)$ (inset of Fig. 1). This means that the wavepacket for species m will propagate along y with mean velocity $v_m = k_0/m$, and its center will arrive at the screen at $y = L$ in time $t_m = mL/k_0$. Although time evolution entangles the internal and translational modes so that $\psi_m(t, \mathbf{x})$ is mass dependent, the wavefunctions at their respective t_m does not depend on mass

$$\psi_m(t_m, \mathbf{x}) = \sqrt{\frac{k_0}{2\pi i L}} \int d^3\mathbf{x}'\, e^{-\frac{k_0(\mathbf{x}-\mathbf{x}')^2}{2iL}}\psi_{\rm ini}(\mathbf{x}') \equiv \psi_{\rm fin} \qquad (2)$$

In other words, the mass dependence of propagation and time of arrival cancel each other, so that all species have the same wavefunction upon arrival at the screen. Therefore, the pattern registered by the screen for each species will be the same modulo spatial displacement.

The Measurement Process.– For each species, we measure the number of particles captured by the screen per area over the lifetime of the experiment. We call this quantity the areal density and denote it by σ_m, and our final outcome σ is the sum of σ_m over the mass distribution. To calculate σ_m, we introduce the 4-current operator $\hat{j}^\nu_m(x^\mu) = i\left[\partial^\nu\hat{\phi}_{m,-}(x^\mu)\right]\hat{\phi}_{m,+}(x^\mu) + h.c.$, where we've defined $\hat{\phi}_{m,+}$ and $\hat{\phi}_{m,-}$ as the positive and negative frequency components of $\hat{\phi}_m$. For a particular quantum state $|\Psi\rangle$, $\langle\Psi|\hat{j}^\nu_m(x^\mu)|\Psi\rangle$ represents the 4-probability current for species m. Then the number of particles in a spacetime volume V is given by the flux integral

$$N_m[V] = \int_V d\Sigma_\nu \langle \Psi_m | \hat{j}^\nu_m | \Psi_m \rangle \,. \tag{3}$$

For N_m counted by a particular pixel on the screen, V is spanned by $d\Sigma_\nu$, which is the differential volume one-form corresponding to the proper area and proper time for the pixel. This quantity depends on the detector trajectory, which we will now characterize.

Detector Trajectory.– We allow the screen to move arbitrarily along z, and we parametrize its *central pixel* by its proper time τ

$$x^\mu_{\rm cs} = [t_{\rm cs}(\tau), 0, L, z_{\rm cs}(\tau)] \tag{4}$$

The central pixel has instantaneous 3-velocity $\beta(\tau)$ and Lorentz factor $\gamma(\tau)$, and its proper acceleration is given by $g = \gamma^2 d\beta/d\tau$. To find $d\Sigma_\nu$, we establish a *proper reference frame* [15] for the central pixel with coordinates (τ, X, Y, Z) , which maps to Minkowski as

$$x^\mu(\tau, X, Y, Z) = [t_{\rm cs}(\tau) + \beta\gamma Z, X, Y + L, z_{\rm cs}(\tau) + \gamma Z] \tag{5}$$

We note that when g is constant, Eq. (5) recovers the transformation to Rindler coordinates. In this coordinate system, pixels on the screen are parametrized spatially by (X, Z), with $Y = 0$. Then, the differential volume one-form at (X, Z) is given in Minkowski coordinates by $d\Sigma_\nu(X, Z) = [0, 0, (1 + gZ)dXdZd\tau, 0]$. Using Eq. (3) and averaging over area, we obtain the areal density for each species

$$\sigma_m(X, Z) = \int d\tau \, (1 + gZ) \langle \Psi_m | \hat{j}^y_m \left(x^\mu(\tau, X, 0, Z)\right) | \Psi_m \rangle \tag{6}$$

Finally, the total count per area is given by integrating over the mass distribution P_m, so that $\sigma(X, Z) = \int dm \; P_m \sigma_m(X, Z)$.

The Interference Pattern and Loss of Visibility.– We will now evaluate (6) by making some simplifying approximations: since $f_m(\mathbf{k})$ is localized around $\bar{\mathbf{k}}$, and further assuming that the packets are spatially localized to within $l \ll L$, where L is the propagation distance, we can write Eq. (6) as a *spatial* integral of $|\psi_m(t_m)|^2 = |\psi_{\rm fin}|^2$ along y. These approximations correspond to the physical picture that the wavepacket dynamics is semiclassical along the propagation direction, and that it passes through the screen in a short enough time so that during measurement, the packet shape is approximately rigid. We emphasize that for all species, we integrate over the same wavefunction $\psi_{\rm fin}$. However, $\sigma_m(X, Z)$ is still mass dependent, but this dependence is now incorporated into the integration trajectory in the y-z plane along which the pixel (X, Z) samples $|\psi_{\rm fin}|^2$. For our assumptions, the effect of this trajectory is well approximated by the position at which the pixel samples $|\psi^2_{\rm fin}|$ at the particular time of arrival t_m for each species m. If we additionally assume wavefunction separability such that $\psi_{\rm fin}(x, y, z) = \psi^x_{\rm fin}(x)\psi^y_{\rm fin}(y)\psi^z_{\rm fin}(z)$, and non-relativistic velocities for the screen such that $\gamma \approx 1$, Eq. (6) reduces to the physically the physically intuitive form

$$\sigma_m(X, Z) = \left|\psi^x_{\rm fin}(x)\right|^2 \left|\psi^z_{\rm fin}[\tilde{z}_{\rm cs}(t_m) + Z]\right|^2 \tag{7}$$

where $\tilde{z}_{\rm cs}(t)$ is an explicit function of t that gives the central pixel's z position in Minkowski time. Simply put, since each species has a different time of arrival, then the pattern registered by a screen moving along z will have a m-dependent spatial shift, as shown in Fig. 2. This mass dependence is shown explicitly in Eq. (7) through $\tilde{z}_{\rm cs}(t_m)$.

To see how this causes loss of fringe visibility, suppose now that $\psi^z_{\rm fin}$ contains an interference pattern with visibility V, so that locally around $z \approx \tilde{z}_{\rm cs}(t_m)$ we have $|\psi^z_{\rm fin}(z)|^2 \propto [1 + V\cos(\alpha z + \phi)]$, where α is the wavenumber of the spatial oscillation. We can ignore ϕ without loss of generality, and write

$$\sigma(Z) \propto \int P_m \left(1 + V\cos[\alpha z_{\rm cs}(t_m) + Z]\right) dm \tag{8}$$

This is simply a sum of shifted cosines, which will result in an "fuzzy" interference pattern with a new visibility V' such that

$$\frac{V'}{V} = 1 - \frac{\alpha^2 \dot{\tilde{z}}^2_{\bar{m}} t^2_{\bar{m}}}{2} \left(\frac{\Delta m}{\bar{m}}\right)^2 \tag{9}$$

where Δm^2 is the variance of the mass distribution, $\bar{m}$ is the average mass and the $\bar{m}$ subscript is used denote quantities of the average mass particle. We emphasize that the loss of contrast we predict depends crucially on the transverse *velocity* of the screen at time $t_{\bar{m}}$, denoted by $\dot{\tilde{z}}_{\bar{m}}$, and has no dependence on the *acceleration*, or equivalently, on gravity.

Note that Eq. (9) assumes small differences in spatial shifts between species compared the coherence lengthscale, corresponding to short measurement times. But since the interference pattern is just the superposition of shifted cosines, for finite number of particle species, we can always find a time at which the oscillations for all species have cycled over an integer number of 2π. This will recover full fringe visibility, and corresponds to the "revival" effect of Ref. [1].

A Double Slit Experiment in a Uniformly Accelerating Lab.– We now apply our model to the specific thought experiment of Ref. [1], where there is an initial spatial superposition of the translational mode so that $\psi_{\rm ini}(x, y, z) \propto [\delta(z - z_1) + \delta(z - z_2)]$, and a thermal distribution at high temperature T of N harmonic DOF's, being measured by a detector with uniform acceleration g. From this, we calculate the parameters $V = 1$ and $\alpha = k_0(z_1 - z_2)/L$ from $\psi_{\rm fin}$, $\tilde{z}_{\rm cs}(t) = gt^2/2$ and $\dot{\tilde{z}}_{\bar{m}} = gt_{\bar{m}}$ from the detector motion, and $\Delta m = k_B T\sqrt{N}$ from the mass distribution. Inserting these into our general result in Eq. (9), we find

$$V' = 1 - \frac{N}{2}\left[g(z_1 - z_2)k_B T\right]^2 t^2_{\bar{m}} \tag{10}$$

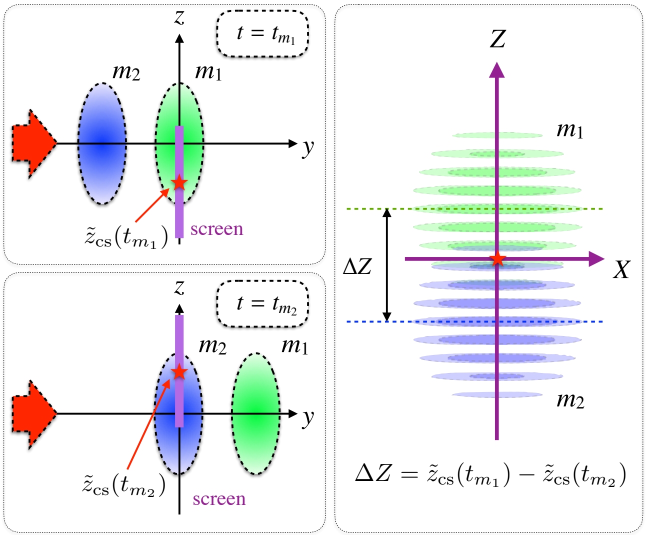

FIG. 2: Snapshots taken upon arrival of m_1 and m_2 ($m_1 < m_2$) packets at the screen, at t_{m_1} (upper left panel) and t_{m_2} (lower left panel), respectively (separation between the packets highly exaggerated). Positions of the screen differ at these moments (with central pixel labeled by red star), causing a shift in the interference pattern registered by the screen, which is best viewed in the central pixel's proper reference frame (right panel).

which exactly reproduces the loss of contrast found in Ref. [1]. Using the insight that this is a kinematic effect which is due to a coordinate transformation, we now address this thought experiment without extension to our physical model to establish direct correspondance.

The (1+1)d thought experiment.– We briefly state results from the thought experiment of Ref. [1] using our kinematic interpretation. Here, state preparation and detection occurs in two different Local Lorentz frames, which we denote by LLF-E for the emitter and LLF-D for the detector, with coordinates (t, z) and (τ, Z) respectively. Here, detection at time τ is an instantaneous evaluation of the particle's wavefunction in LLF-D. Mapping the initial wavefunction $\psi_m(0) \propto [\delta(z - z_1) + \delta(z - z_2)]$ in LLF-E to a state vector, we boost the field operator $\hat{\phi}_m$ by the instantaneous velocity v of LLF-D at detection time. The spatial distribution in LLF-D at τ for species m is then

$$|\psi_m(\tau, Z)|^2 \propto 1 - \cos\left[\frac{m}{\tau}(Z - z_c + v\tau)\,\Delta z\right] \tag{11}$$

where $\Delta z = z_2 - z_1$, and $z_c = (z_2 + z_1)/2$ is the center of the superposition. We point out that here the mass dependence lies in the spatial frequency of the interference cosine term, which again can be traced back to de Broglie wave dispersion. The effect of an accelerating detection frame that observes the system at the same coordinate point Z is to observe it at a point farther away from z_c as time increases. In the limit where the detector motion dominates such that $v\tau \gg Z - z_c$, such as when $Z \sim z_1, z_2$ for realizable massive superpositions, and for $v = g\tau$, we obtain the the same loss of contrast as in Ref [1].

Origin of the loss in visibility.– While our predicted loss of visibility in Eq's. (10) for the Eq. (11) the same as that of Ref. [1] in the appropriate limits, we interpret this effect as being unrelated to gravity. The true source of dephasing is the mass dependent dispersion of de Broglie waves. In our experimental particle beam model, this manifests as mass dependent propagation velocities, causing the species to arrive at different times. This implies that a particular pixel on the moving screen is effectively evaluating $\psi_{\rm fin}(\mathbf{x})$ at mass dependent positions along z as shown in Eq. (7) and in the left panels of Fig. 2. On the screen itself, this means that different species land on different locations, resulting in mass-dependent shifts of their interference patterns along Z [Fig. 2, right panel], which in turn smears out the pattern. Pictured in the lab frame, packets of different species separate along y and drop onto the screen at different heights. The size of these shifts, and consequently the dephasing, depends on both the amount of time the species are allowed propagate, as well as the velocity of the screen at measurement time. In this way, the loss of visibility appears as a rate that is directly related to the transverse *velocity* of the detector [Eq. (9)], instead of *acceleration*. In the situation considered by Ref. [1], gravity happens to supply such a transverse velocity, thereby making the decrease in visibility dependent upon the gravitational acceleration. However, if we give the screen a uniform velocity in the Lab frame (with gravity) that matches the velocity at which the packets fall in the lab frame, there will be no loss of visibility. *Vice versa*, even in absence of gravity, any motion of the screen transverse to the beam's propagation direction as the packets land will lead to a loss of visibility. As for the thought experiment of Ref. [1], mass dependent wave dispersion implies greater dephasing among different species in regions farther away from the center of the initial superposition. Observing interference at constant lab coordinates equates to observing the system at a point whose distance from its center increases with time, resulting in an apparent dephasing "rate". Thus, our formalism offers an alternative perspective that the loss of visibility is a is a *kinematic effect* instead of a gravitational one.

Conclusions.– Having treated both the thought experiment of Ref. [1] and its possible physical implementation as a particle beam interferometry experiment, in both cases we offer the point of view that dephasing between different internal states do not arise from gravity, but instead from the mass dependence of their de Broglie waves' dispersion and the relative transverse motion of the detector. Furthermore, the dephasing we calculate from this perspective is the same as that predicted by Ref. [1] using their perspective of time dilation [18]. In these calculations, we have assumed EEP to be valid. The comparison of these two approaches - by treating gravity explicitly versus as acceleration - offers possibilities to study the implications of EEP in quantum systems and to test for its violations in this regime. To do this, we will have to consider a more general Hamiltonian in the Lab frame

$$\hat{H} = \hat{\mathbf{p}}^2/(2\hat{M}) + \hat{\mathbf{G}} \cdot \hat{\mathbf{x}} \tag{12}$$

where $\hat{\mathbf{G}}$, the gravitational force, is no longer given by $\hat{M}\mathbf{g}$, which would *a priori* be consistent with Weak Equivalence. In this case, the packets of multiple mass components will separate due to both the spectrums of $\hat{M}$ and $\hat{\mathbf{G}}$, and now gravity will cause packet separation in addition to the effect of mass. It is also plausible that preparation of novel quantum states can reveal more structures in the operator $\hat{\mathbf{G}}$ that could otherwise be revealed by a classical experiment [16],[17].

Acknowledgements.– Research of Y.C. and B.P. are supported by the Institute for Quantum Information and Matter, as we as NSF Grants PHY-1404569 and PHY-1506453. Research of F.K. was supported by LIGO NSF Grant PHY-1305863 and Russian Foundation for Basic Research Grant 14-02-00399. We thank C. Brukner, I. Pikovski, Y. Ma, B.L. Hu and O. Romero-Isart for exciting discussions.

[1] I. Pikovski, M. Zych, F. Costa, and C. Brukner, Nature Physics **11**, 668 (2015).
[2] H. Yang, H. Miao, D.-S. Lee, B. Helou, and Y. Chen, Physical review letters **110**, 170401 (2013).
[3] I. Pikovski, M. R. Vanner, M. Aspelmeyer, M. Kim, and Č. Brukner, Nature Physics **8**, 393 (2012).
[4] D. E. Bruschi, T. C. Ralph, I. Fuentes, T. Jennewein, and M. Razavi, Physical Review D **90**, 045041 (2014).
[5] M. Zych, F. Costa, I. Pikovski, T. C. Ralph, and Č. Brukner, Classical and Quantum Gravity **29**, 224010 (2012).
[6] J. F. Donoghue, Physical Review D **50** (1994).
[7] M. P. Blencowe, Physical Review Letters **111** (2013).
[8] L. Diósi, Physics Letters A **120** (1987).
[9] R. Penrose, General Relativity and Gravitation **28** (1996).
[10] S. Adler and A. Bassi, Physics Letters A **380** (2016).
[11] L. Diósi, arXiv preprint arXiv: 1507.05828 (2015).
[12] Y. Bonder, E. Okon, and D. Sudarsky, Physical Review D **92** (2015).
[13] I. Pikovski, M. Zych, F. Costa, and Č. Brukner, arXic preprint arXiv:1508.03296 (2015).
[14] C. M. Will, Living Rev. Relativity **4** (2014).
[15] C. W. Misner, K. S. Thorne, and J. A. Wheeler, *Gravitation* (Macmillan, 1973).
[16] L. Viola and R. Onofrio, Physical Review D **55**, 455 (1997).
[17] M. Zych and Č. Brukner, arXiv preprint arXiv:1502.00971 (2015).
[18] The authors of Ref. [1] hold the position that the effect they describe is due to time dilation, and thus a different effect than discussed here.